Comparison of Drop Size Distribution Measurements by Impact and Optical Disdrometers

ALI TOKAY

Joint Center for Earth Systems Technology, University of Maryland, Baltimore County, Baltimore, Maryland

ANTON KRUGER AND WITOLD F. KRAJEWSKI

Iowa Institute of Hydraulic Research, The University of Iowa, Iowa City, Iowa

(Manuscript received 25 October 2000, in final form 30 May 2001)

ABSTRACT

Simultaneous observations made with optical- and impact-type disdrometers were analyzed to broaden knowledge of these instruments. These observations were designed to test how accurately they measure drop size distributions (DSDs). The instruments' use in determining radar rainfall relations such as that between reflectivity and rainfall rate also was analyzed. A unique set of instruments, including two video and one Joss–Waldvogel disdrometer along with eight tipping-bucket rain gauges, was operated within a small area of about 100×50 m^2 during a 2-month-long field campaign in central Florida. The disdrometers were evaluated by comparing their rain totals with the rain gauges. Both disdrometers underestimated the rain totals, but the video disdrometers had higher readings, resulting in a better agreement with the gauges. The disdrometers underreported small- to medium-size drops, which most likely caused the underestimation of rain totals. However, more medium-size drops were measured by the video disdrometer, thus producing higher rain rates for that instrument. The comparison of DSDs, averaged at different timescales, showed good agreement between the two types of disdrometers. A continuous increase in the number of drops toward smaller sizes was only evident in the video disdrometers at rain rates above 20 mm h^{-1}. Otherwise, the concentration of small drops remained the same or decreased to the smallest measurable size. The Joss–Waldvogel disdrometer severely underestimated only at very small drop size (diameter $\leq$ 0.5 mm). Beyond the Joss–Waldvogel disdrometer measurement limit were very large drops that fell during heavy and extreme rain intensities. The derived parameters of exponential and gamma distributions reflect the good agreement between the disdrometers' DSD measurements. The parameters of fitted distributions were close to each other, especially when all the coincident measurements were averaged. The low concentrations of very large drops observed by the video disdrometers did not have a significant impact on reflectivity measurements in terms of the relationships between reflectivity and other integral parameters (rain rate, liquid water content, and attenuation). There was almost no instrument dependency. Rather, the relations depend on the method of regression and the choice of independent variable. Also, relationships derived for S-band radars and Tropical Rainfall Measuring Mission (TRMM) precipitation radar (PR) differ from each other primarily because of the higher reflectivities at the shorter PR wavelength at high rain-rate regime.

1. Introduction

Measurements of the drop size distribution (DSD) have a broad range of applications in meteorology, hydrology, and related sciences. In particular, accurate estimates of areal rainfall through radar measurements benefit from the knowledge of the drop size distribution. In principle, the use of radar requires a relationship between its measured reflectivity Z and the estimated rainfall R. Such a relationship, known as Z–R, can be derived from long-term observations of DSDs using disdrometers. The ''goodness'' of the relation can be evaluated by comparing the radar rainfall with in situ rain gauge measurements. If the radar operates at high frequencies, one should take into account attenuation A of the radar signal. The attenuation is also a function of DSD, and A–Z relations also can be derived from disdrometer measurements.

The characteristics of an averaged DSD, which represents a precipitation type in a climatological region, are important for cloud-modeling studies. For example, Ferrier et al. (1995) showed that models that simulate clouds exhibit differences in the vertical profile of rain and the lateral extent of the stratiform rain in oceanic convection due to variations in the DSD parameterization. Because cloud models are used in passive microwave satellite-based rainfall retrieval algorithms,

Corresponding author address: Dr. Ali Tokay, NASA Goddard Space Flight Center, Code 912, Greenbelt, MD 20771.
E-mail: tokay@radar.gsfc.nasa.gov

TABLE 1. Variables of product a and X and their units corresponding to the integral rain parameters P that are directly calculated from Joss–Waldvogel disdrometer measurements by using Eq. (1). The integral rain parameters are rain rate R, concentration C, liquid water content M, reflectivity in Rayleigh scattering regime Z, reflectivity in Mie scattering regime Z_e, and attenuation A. The variables are described in the text.

P	a	X	Units
R (mm h^{-1})	$6 \times 10^{-4}\ \pi/(\tau\alpha)$	D^3	τ (s), α (m^2), D (mm)
N (m^{-3})	$1/(\tau\alpha)$	$1/v_T$	τ (s), α (m^2), v_T (m s^{-1})
M (g m^{-3})	$\rho_w\ 10^{-3}\pi/(6\tau\alpha)$	D^3/v_T	ρ_w (g cm^{-3}), τ (s), α (m^2), D (mm), v_T (m s^{-1})
Z (mm^6 m^{-3})	$1/(\tau\alpha)$	D^6/v_T	τ (s), α (m^2), D (mm), v_T (m s^{-1})
Z_e (mm^6 m^{-3})	$10^6\lambda^4/(\pi^5\|K\|^2\tau\alpha)$	σ_b/v_T	λ (mm), τ (s), α (m^2), σ_b (m^2), v_T (m s^{-1})
A (dB km^{-1})	$4343/(\tau\alpha)$	σ_{ex}/v_T	τ (s), α (m^2, σ_{ex} (m^2), v_T (m s^{-1})

DSD therefore plays a significant role in their calibration (Hong et al. 1999).

The various applications of DSD, noted above, are key objectives of the National Aeronautics and Space Administration's (NASA) Tropical Rainfall Measuring Mission (TRMM). TRMM aims to produce a four-dimensional latent heating profile in the Tropics. As the TRMM satellite flies over the tropical belt, 70% of which is covered by the oceans, it provides estimates of surface precipitation through its active and passive sensors (Kummerow et al. 1998). TRMM's ground validation program, on the other hand, continuously monitors the surface rainfall at selected sites. A major objective of the ground validation program is to evaluate satellite rainfall products in different climatic regions. To this end, NASA conducted five field campaigns between March of 1988 and September of 1999 in various places around the Tropics. In this study, we analyzed the DSD observations collected during the TRMM field campaign called the Texas–Florida Underflight-B (TEFLUN-B) experiment in central Florida. The DSD observations are from a Joss–Waldvogel disdrometer (JWD), and a new instrument, a two-dimensional video disdrometer (2DVD). Our main aim is to communicate the results of the instrument intercomparison, with implications for the accuracy of the measurements of the DSD and the associated bulk descriptors of rainfall.

We have organized the paper as follows: in section 2 we review the ground-based disdrometers. In section 3 we present the characteristics of rainfall observations by the collocated disdrometers and tipping-bucket rain gauges. In section 4 we focus on the simultaneous observations of DSD by the two collocated disdrometers, and in section 5 we illustrate the differences in the characteristics of the averaged DSD. In section 6 we investigate the instrument and DSD-estimation-method sensitivities with respect to the reflectivity–rainfall and other similar relationships. In the last section, we summarize the findings and offer concluding remarks.

2. Disdrometers

Since Joss and Waldvogel (1967) introduced an electromechanical disdrometer, the number of observational studies of the drop size distribution underwent an exponential growth. Many studies (e.g., Sauvageot and Lacaux 1995; Tokay and Short 1996) on the evolution of droplet spectra, parameterization of the DSD, and development of the empirical relations between various rain parameters rely on observations from the JWD. Prior to JWD, the collection of large samples of raindrop images using an automated camera in ten different locations was probably the most comprehensive measurement of DSD (Jones 1992). Marshall and Palmer (1948), who were pioneers in DSD parameterization, used samples of raindrop records on dyed paper filters collected by Laws and Parsons (1943) and Marshall et al. (1947).

The JWD, which has been commercially available for over 30 years, was originally designed for the purpose of calculating radar reflectivity. It is an impact-type device and measures the drop size with about 5% accuracy. The JWD has a sampling cross-sectional area of 50 cm^2, and drops are sorted into 20 size intervals ranging from 0.3 to about 5.0–5.5 mm for 30-s averaging periods. The boundaries of the 20 channels are not uniform and increase with drop size from 0.1 to about 0.5 mm. The calibration of each unit determines the exact channel boundaries (Sheppard 1990; McFarquhar and List 1993). In the TEFLUN-B experiment, the output of the JWD, that is, the number of counts in each of 20 channels, was averaged over 1-min intervals. The minutes that recorded less than 10 drops or a rain rate of less than 0.1 mm h^{-1} are considered to be within the noise level and are disregarded.

The integral rain parameters P that are of interest in this study are then directly calculated from JWD spectra and can be represented by the form

$$P = a \sum_{i=1}^{20} C_i X_i, \tag{1}$$

where a is the product of parameters that are invariant with drop size, C_i is the number of drops in the ith channel, and X_i is the moment of the middle drop size of the ith channel, and/or a parameter that varies with drop size. Table 1 lists the variables of the product a and the moment X corresponding to the integral rain parameters rain rate, drop concentration, liquid water content, radar reflectivity in Rayleigh scattering regime, radar reflectivity in Mie scattering regime, and attenuation. The units of integral parameters and all the var-

iables also are given in Table 1. The disdrometer's sampling cross section α and sampling time τ are fixed variables that appear in all equations. The density of water ρ_w, another fixed variable, appears only in liquid water content. The terminal fall speed of raindrops v_T, which increases nonlinearly with drop size, is calculated for midsize diameters of each channel following the measurements of Gunn and Kinzer (1949, hereinafter GK). The reflectivities are further converted to reflectivity decibel (dBZ) units.

For a radar that operates at short wavelengths λ ($\leq$5 cm), reflectivity is calculated more accurately using the formulas of the Mie scattering regime and is expressed as a function of DSD and backscattering cross section σ_b. The backscattering cross section is calculated for the midsize diameters of the size intervals and is a function of wavelength and temperature. Of particular interest, the wavelength of the TRMM precipitation radar (Kummerow et al. 1998), $\lambda = 21.7$ mm, is employed in this study. The reflectivity in the Mie scattering regime is also function $|K|^2 = |(m^2 - 1)/(m^2 + 2)|^2$, where m is the complex refractive index of water. At these short wavelengths, backscattering power is attenuated prior to reaching the radar. The attenuation is a function of the extinction cross section σ_{ex}. Like σ_b, σ_{ex} is calculated for middle diameters of the size intervals and is a function of temperature and wavelength.

The JWD is a reliable instrument that operates continuously and unattended. Nevertheless, it has some shortcomings. It underestimates the number of small drops in heavy rain because of ringing of the styrofoam cone when it is hit by the drops. This is known as disdrometer dead time, and to correct for it the manufacturer supplies a correction matrix (Sheppard and Joe 1994). However, if there are no drops in a given channel, the correction matrix does not add any drops; rather, it modifies the DSD and increases the high moments of the drop size such as rain rate significantly. This fact is a problem of the correction matrix, and therefore many users choose not to implement it (Tokay and Short 1996). The JWD should be deployed in a noise-free environment, or otherwise small drops cannot be distinguished from the acoustic background noise. At the large drop end, drops larger than 5.0–5.5-mm diameter cannot be resolved at their true size; rather, they are assigned to the largest size bin.

The JWD assumes that the drops fall at their terminal fall speed. The disdrometer's output pulse is proportional to the size and fall speed of the impacting drops. The size of the impacting drop is retrieved from an output pulse using a relation between fall speed and drop diameter in still air derived from observations by GK. In the presence of updrafts and downdrafts, the assumption of terminal fall speed can result in erroneous drop sizes.

The developments of optical disdrometers by which both size and fall speed of the drops are measured brought a new perspective on the influence of updrafts and downdrafts on falling raindrops (Donnadieu 1980; Stow and Jones 1981; Hauser et al. 1984). Donnadieu studied the errors in the size measurements of JWD using collocated JWD and optical spectropluviometer observations. He found that, on average, the drops were falling faster than in the GK observations. Therefore, the sizes of the drops were less than that reported by JWD. Hauser et al. (1984) and Stow and Jones (1981) also showed that fall speeds of raindrops differ from terminal fall speed. Hosking and Stow (1991) reported that, on average, drops fall about 5% to 10% slower than their terminal fall speed, and the mean deviation increased with drop size.

Despite advances in disdrometer technology in the 1980s, the JWD is still considered to be the *standard* for DSD measurements at the ground surface. Recently, an optical disdrometer, known as a two-dimensional video disdrometer, became commercially available. The 2DVD measures not only drop size and fall velocity but also drop shape. It is a delicate electronic optical device that requires frequent attendance. The components and measuring principles of the 2DVD can be found in Schönhuber et al. (1997). In short, the disdrometer consists of outdoor sensor and electronics units and an indoor user terminal. The image of the falling drop is scanned twice in two planes separated by about 6 mm. The distance between the two planes is used to determine the fall speed of the drops. To determine the size of the drop, a matching algorithm is applied among the drops in two planes. The equivalent diameter of the drop is then determined from the drop volume.

The 2DVD has been employed in recent field studies of ice and raindrop physics (Barthazy et al. 1998; Tokay et al. 1999; Schuur et al. 2001). It has 2 times the sampling area of the JWD and can measure the size of the drops with the nominal accuracy of $\pm$0.2 mm. To calibrate the instrument, a user drops metal balls ranging in size between 0.5 and 10 mm into the orifice. Through experience, we determined that drops smaller than 0.2 mm are unreliable; therefore, we disregarded them in this study. We calculated the integral parameters for each minute of observations using Eq. (1), with two exceptions: 1) we used the measured size of the drop rather than midsize bin, and 2) we used the measured fall speed of the drops. We constructed the DSD for 1-min periods, adopting a 0.2-mm channel interval from 0.2 to 8.0 mm. We disregarded the minutes that had fewer than 10 drops or rain rates of less than 0.1 mm h^{-1}.

The 2DVD occasionally records spurious small drops. Although a Velcro-type splash guard material is placed around the orifice to reduce splashing, it becomes less effective in heavy rainfall as it saturates with water. The splashing generates drops that enter the sensing area. In addition, the mismatch of drops registered by the two cameras in heavy rain is not uncommon. In windy conditions, small drops may pass the observing area at low angles without falling into the container (Nešpor et al. 2000). These spurious drops result in false terminal fall

TABLE 2. Rain accumulation statistics for the Joss–Waldvogel disdrometer and for eight tipping-bucket rain gauges. The $\langle RA_{JWD} \rangle$ and $\langle G \rangle$ denote the mean rain total of Joss–Waldvogel disdrometer and rain gauge, respectively.

Gauge No.	No. of rain events	$\langle RA_{JWD} \rangle$ (mm)	$\langle G \rangle$ (mm)	Percentage of mean standard error
1	33	7.97	10.72	23%
2	24	8.17	10.61	18%
3	24	8.17	10.33	18%
4	26	7.86	9.69	14%
5	29	7.12	9.06	19%
6	28	7.34	11.79	27%
7	31	8.32	10.04	14%
8	29	8.84	10.54	9%

TABLE 3. Rain accumulation statistics for the UI video disdrometer and for eight tipping-bucket rain gauges. The $\langle RA_{2DVD} \rangle$ and $\langle G \rangle$ denote the mean rain total of UI video disdrometer and rain gauge, respectively.

Gauge No.	No. of rain events	$\langle RA_{2DVD} \rangle$ (mm)	$\langle G \rangle$ (mm)	Percentage of mean standard error
1	13	9.74	12.13	14%
2	12	9.08	11.49	11%
3	12	9.08	11.20	8%
4	13	9.13	10.59	10%
5	12	9.80	10.94	10%
6	13	9.74	12.43	16%
7	13	9.74	10.92	12%
8	13	9.74	10.41	15%

speeds. We adopted a threshold of fall speed to filter out the spurious drops using GK results, as did other researchers in the previous studies. Donnadieu (1980), for instance, filtered out drops beyond ± 1 m sec^{-1} of GK observations, retaining 76% of the drops. Hauser et al. (1984), on the other hand, retained the drops within $\pm 50\%$ of GK observations, excluding 12% of the drops. In this study, we adopted a $\pm 50\%$ threshold because the size of the spurious drops is typically less than 2 mm in diameter. This choice eliminates 18% of the observations.

3. Rainfall measurements

The rainfall measurements presented here were collected during a field campaign in central Florida. During the Florida phase of TRMM's TEFLUN-B field campaign, a JWD was operated 68 days, starting from 21 June 1998. The JWD was placed within a dense surface rain gauge network and close to two 2DVDs, a profiler pair, and eight tipping-bucket rain gauges. This site was designated as the master site of the dense rain gauge network and covered an area of about 100×50 m^2. The JWD was operated almost uninterruptedly, collecting 274 mm of rainfall in 49 rainy hours. Although 77% of the time rain was at rain rates less than 5 mm h^{-1}, 84% of the total rain fell above the 5 mm h^{-1} threshold. About 50% of the rain events lasted less than 15 min, and 17% of the rain events were longer than 1 h. We define a rain event based on at least one rainy minute in 15 consecutive minutes.

We examined the performance of the JWD by comparing its estimates of the rain totals with those of the rain gauges. In Table 2, we present the percentage of mean standard errors of JWD with regard to each nearby gauge, assuming the rain gauge error is negligible (Habib et al. 1999, 2001). These statistics are based on rain events with at least 1-mm rain totals. The percentage error of JWD rainfall was about 18% on average, with a standard deviation of $\pm 5\%$ (Table 2). All the gauges but two were at ground surface: gauge 1 was located on the roof of a 2.5-m-high trailer, and gauge 7 was atop a 2-m-high post. The gauges were located in pairs set 1 m apart: 2 and 3, 4 and 5, and 7 and 8. Gauges 1–3 were within a few meters of the JWD; gauge 6 was farthest away from the JWD. In Tables 2 and 3, we also include the number of coincident rain events and mean JWD and gauge rainfall.

The rain total by JWD was less than the rain total observed by any gauge in every rain event. As an example, Fig. 1a shows a 1-to-1 comparison of rain totals from JWD and gauge 1. This result is partially due to the underestimation of drops at diameters less than 1.1 mm in JWD. The limit of maximum drop sizes may also play some role.

The video disdrometers were provided by The University of Iowa (UI) and the TRMM office of NASA Goddard Space Center. The UI and NASA video disdrometers were located side by side, with the first operating for 41 noncontiguous days and the second for 18. The high humidity and air temperature were the leading cause for frequent failure of the instruments. There were 13 and 5 rain events where the rain gauges had at least 1 mm of rainfall measured by UI's and NASA's 2DVD, respectively. Because of the insufficient number of cases, the rain accumulation statistics between the NASA 2DVD and nearby gauges were not studied. The percentage error of UI 2DVD was 12% on average, with a standard deviation of $\pm 3\%$ (Table 3). A better agreement between 2DVD and gauge rain totals than between JWD and gauge rain totals was evident. The 2DVD mostly underestimated the rain totals (Fig. 1b), due mainly to the mismatched drops that have been eliminated through the velocity threshold mentioned above.

4. DSD observations

a. Past studies

Although numerous studies of drop size distribution used various types of disdrometers, only a few compared the simultaneous measurements of drop size distributions by collocated disdrometers. Donnadieu (1980) pre-

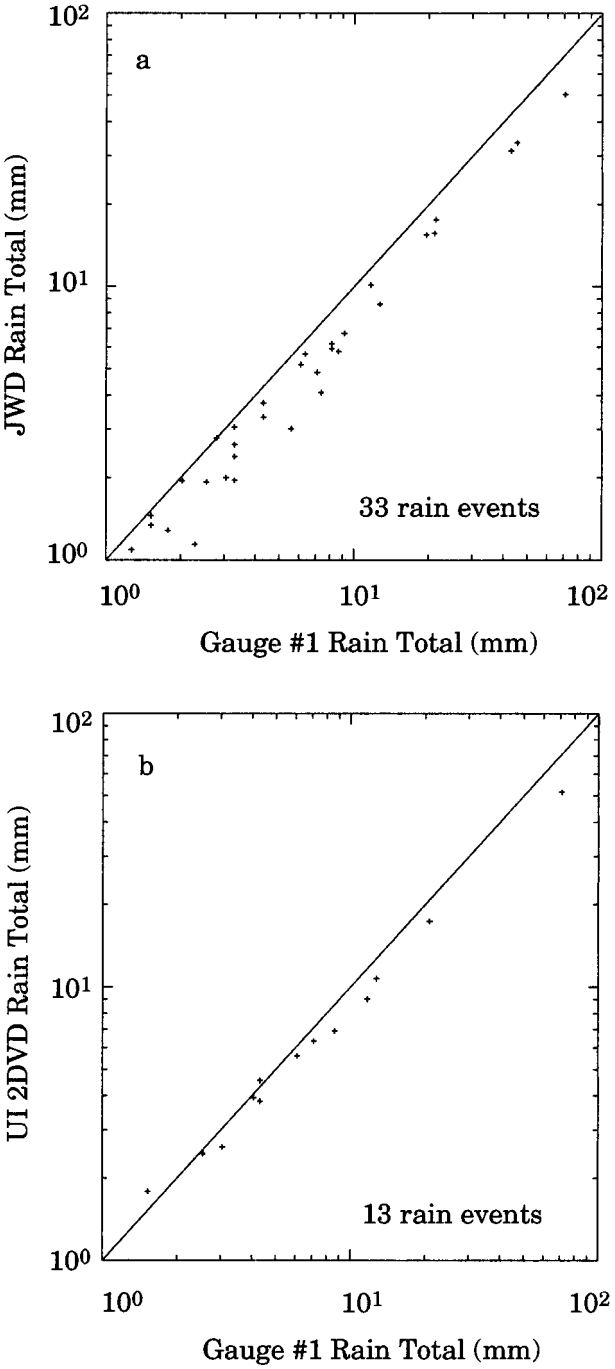

FIG. 1. Event-basis rainfall accumulation measured by the (a) JWD and (b) UI 2DVD in comparison with the gauge 1. The number of rain events is also given.

sented 14 min of composite drop size distributions from simultaneous observations of JWD and an optical disdrometer. He included a size range of between 0.8- and 2.8-mm diameter, resulting in a mean rain rate of 2–4 mm h^{-1}. His results showed the presence of more drops in JWD except in the very first size range [Fig. 1 of Donnadieu (1980)]. Therefore, the integral parameters such as concentration, rain rate, and reflectivity were higher in the JWD than in the optical disdrometer. Loeffler-Mang and Joss (2000) compared 10 min of composite drop size distributions from simultaneous observations of collocated optical disdrometer and JWD. They reported a good agreement between measurements of optical disdrometers and JWDs from the drop size of 0.7–2.0-mm diameter. The presence of more drops in the range from 1.5- to 2.8-mm diameter in JWD measurements suggests higher rain rate and reflectivity in JWD. Having many more drops in sizes less than 0.7 mm in optical disdrometer measurements, on the other hand, results in higher total concentration in the optical disdrometer [Fig. 3 of Loeffler-Mang and Joss (2000)].

Sheppard and Joe (1994) conducted probably the most comprehensive comparative study of drop size distributions from in situ disdrometer measurements. Their experiment included an optical array probe (Knollenberg 1970), a JWD, and an X-band Doppler radar. Sheppard and Joe (1994) presented simultaneous measurements of drop size distributions at different rain intensities. Of particular interest, Fig. 9 of their study was constructed for 4-min averages in a heavy convective rain. The rain rate calculated from Knollenberg spectra was much less (57%) than rain rate calculated from JWD spectra. This difference was due mainly to deficit of the drops in the 1- to 3-mm size range of the probe spectra. Campos and Zawadzki (2000) used a similar setup but with a different type of optical disdrometer (Hauser et al. 1984) instead of a Knollenberg optical array probe. A close look at 5-min-averaged drop size distributions showed a good agreement among the three different sensors' spectra [Figs. 5 and 6 of Campos and Zawadzki (2000)]. The rain rates in this stratiform rain event were around 2.6–3.0 mm h^{-1}.

b. Case studies

We selected three rain events to present the simultaneous measurements of drop size distributions by JWD and 2DVD. The first rain event occurred on 2 September 1998. It was a convective event with two intensive showers, resulting in 5.8–6.1 mm of rainfall in about 40 min (Fig. 2a) according to the nearby gauges. The JWD measured 5.2 mm of rainfall while both video disdrometers recorded 5.6 mm. The first and second intensive periods for which the rain rates remained above 5 mm h^{-1} lasted 5 and 8 min. The composite DSD derived from these 13 min of observations demonstrated a good agreement among the JWD and two 2DVDs (Fig. 3a). Nevertheless, there were differences in drop concentrations at the small drop-size regime (diameter $D < 1$ mm). These differences are mainly due to the underestimation of small drops by the JWD. The minimum drop-size cutoffs also played a role. The size cutoffs are 0.2, 0.3, and 0.6 mm for NASA 2DVD, JWD, and UI 2DVD, respectively. The size cutoffs of the 2DVDs are determined through their calibration, per-

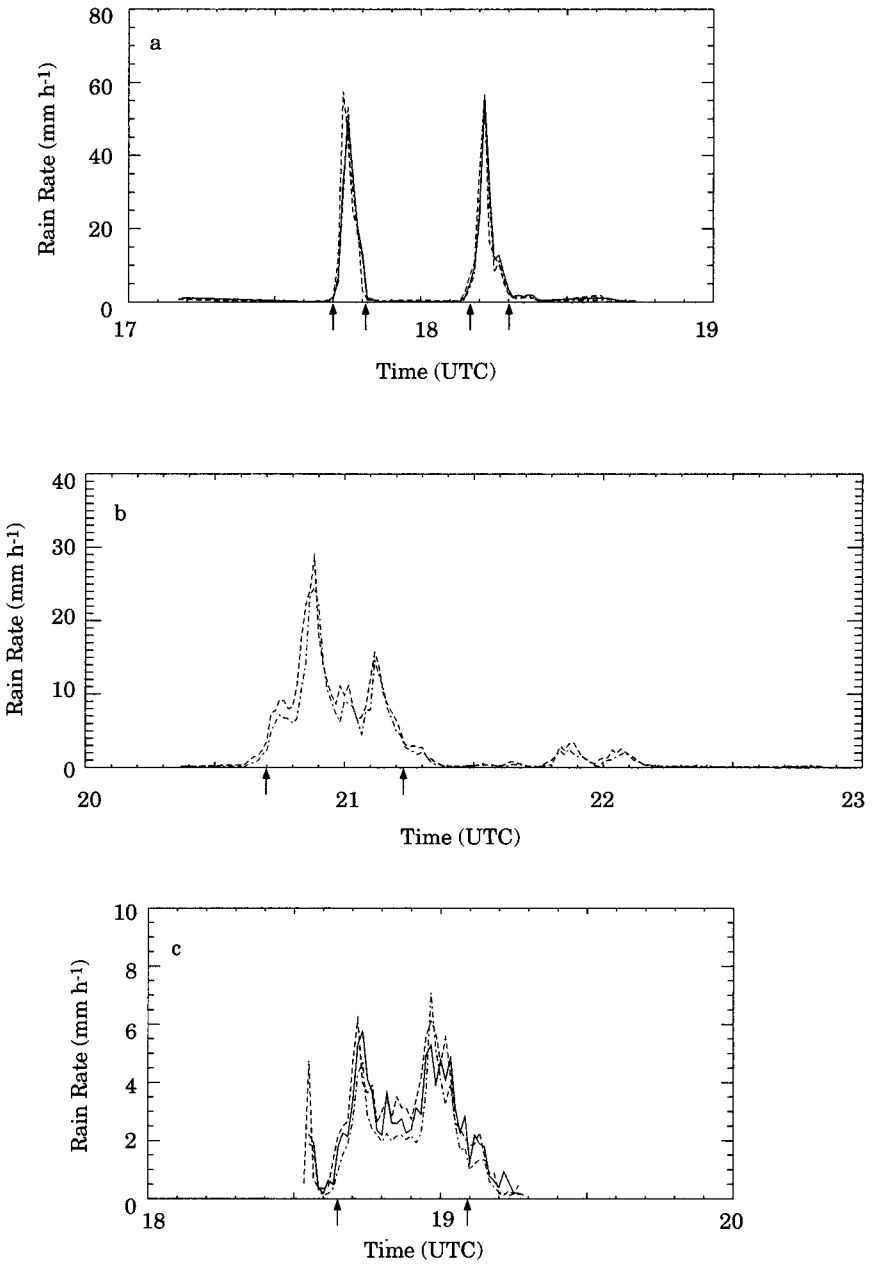

FIG. 2. Time series of rain rate during rain events of (a) 2 Sep 1998, (b) 7 Sep 1998, and (c) 16 Sep 1998. The solid, dashed, and dot–dashed lines represent UI 2DVD, NASA 2DVD, and JWD records, respectively. The arrows denote the time window of the record that was employed for averaging DSD in Fig. 3.

formed utilizing metal balls. The underestimation of small drops in JWD, however, had a limited effect on rain rate and reflectivity because these parameters are related to the higher moments of drop size. The rain rate and reflectivity of JWD spectra were 8% and 1% lower than those from NASA 2DVD.

The second rain event occurred on 7 September 1998. It consisted of a convective shower followed by stratiform rain (Fig. 2b). The rain gauges recorded 6.1–8.1 mm of rainfall in just over 1.5 h. The JWD and NASA 2DVD measured 5.9 and 7.3 mm of rainfall, respectively. The UI 2DVD did not operate in this rain event. During the convective shower, there were 30 consecutive minutes during which rain rates were above 5 mm h^{-1}. The composite DSD derived from this period showed a good agreement between two spectra except for very small drops (Fig. 3b). The underestimation of small drops by JWD is again the main reason for the

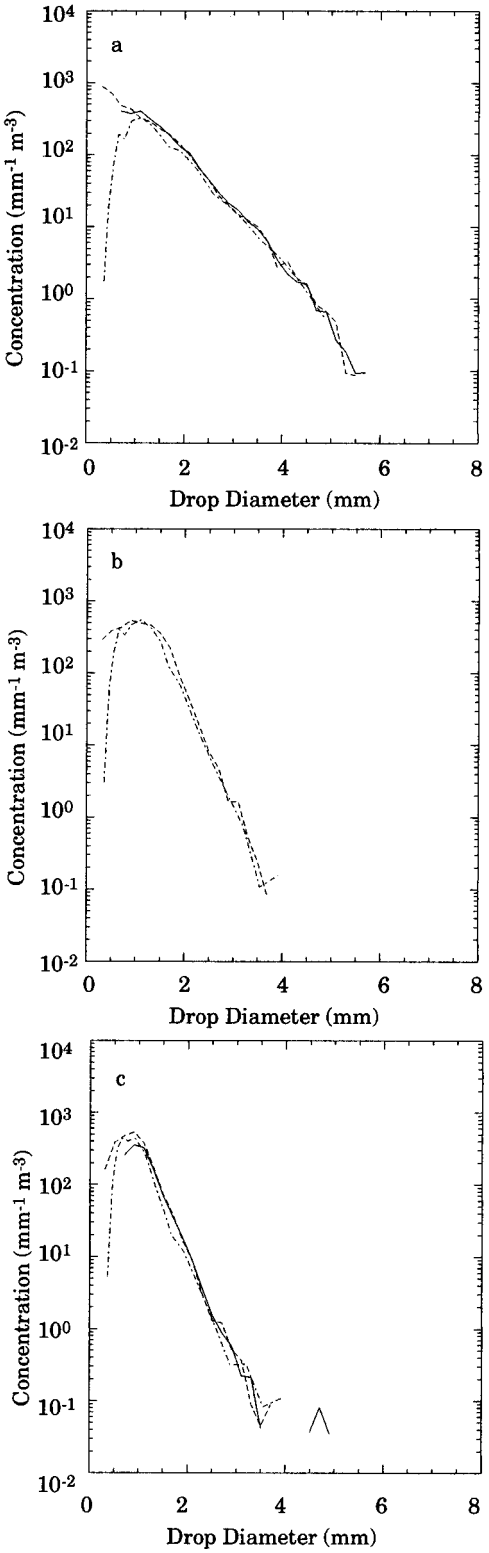

FIG. 3. Averaged drop size distributions for a selected time window in rain events of (a) 2 Sep 1998, (b) 7 Sep 1998, and (c) 16 Sep 1998. The solid, dashed, and dot–dashed lines are the same as identified in Fig. 2.

discrepancy in drop concentrations. The rain rate and reflectivity of JWD spectra were 18% and 3% lower than those from NASA's 2DVD.

The third rain event was on 16 September 1998. It was a stratiform event with the presence of a bright band (Fig. 2c). The rain gauges recorded 1.3–1.8 mm of rainfall in about 45 min. The JWD and NASA 2DVD and UI 2DVD measured 1.5, 2.0 and 1.8 mm, respectively. There were about 27 consecutive minutes during which rain rates were above 2 mm h^{-1}. The composite DSD derived from this period showed good agreement between the two video disdrometers except at the small- and large-size ends of the size spectrum (Fig. 3c). The concentration of the medium-size drops ($1 \leq D < 3$ mm), however, was relatively less in JWD spectra than in the 2DVD spectra. Of interest, there were a few very large drops ($D > 4$ mm) present in UI 2DVD spectra. These drops are probably newly melted drops falling from beneath the cloud base in stratiform rain. The underestimation of small drops by JWD was evident, but only at very small drop sizes ($D < 0.5$ mm). The rain rate and reflectivity of JWD spectra were 30% and 3% lower than those from NASA 2DVD.

To investigate why there were so few small drops in JWD spectra, we used the noise-limit diagram of Joss and Gori (1976). In this diagram, the noise limit is defined as a function of rain rate and drop diameter [Fig. 8 of Joss and Gori (1976)]. At rain rates above 10 mm h^{-1}, 50% of the drop concentration was not detected below a measurable size because of noise from other than environmental sources. For instance, at 20 mm h^{-1}, 50% of the drops cannot be detected below about 0.4 mm because of noise from the following three sources: 1) ringing of the receiving cone after a drop hits the instrument, 2) falling of small splash products formed after the landing of big drops, and 3) acoustic noise of the rain itself in the surrounding environment (Joss and Gori 1976).

In the first rain event, the rain rate calculated from composite JWD spectra (Fig. 3a) was 22 mm h^{-1}. The concentration in NASA's 2DVD was 125% higher than that in JWD, and the difference was due mostly to the underestimation of small drops by the JWD. The rain rate and reflectivity received only 1.8% and 0.1% contribution from small drops. As a result, for these two parameters, the difference between the JWD and NASA 2DVD spectra was insignificant. In the second and third rain events, the rain rates calculated from JWD spectra were 10 (Fig. 3b) and 3 mm h^{-1} (Fig. 3c), respectively. We suspect that, at these rain rates, very small drops are masked by background noise. In these two events, the concentration of drops in JWD was 37% and 28% lower than that of the NASA 2DVD. Again, we attributed the differences to the missing small drops in JWD spectra. Small drops contributed to rain rate and reflectivity in these rain events more than they did in the first event. Nevertheless, the small drops had little impact

on the rain-rate and reflectivity differences between the NASA 2DVD and JWD.

c. Averaged drop size distributions

During TEFLUN-B, there were 1163 and 283 coincident DSD measurements between the JWD and UI 2DVD and between the JWD and NASA 2DVD, respectively. To examine the characteristics of the DSD between the impact and optical disdrometers, we averaged the coincident measurements of the JWD and UI 2DVD for six different rain intensity intervals (Fig. 4) and for the entire dataset (Fig. 5). Because of the limited coincident measurements, no averaging was performed between the JWD and NASA 2DVD. In averaging, we determined the boundaries of rain-intensity intervals based on UI 2DVD measurements. Table 4 presents the percentage contribution of very small ($D < 0.6$ mm), small ($0.6 \leq D < 1$ mm), medium-size ($1 \leq D < 3$ mm), large ($3 \leq D < 5$ mm), and very large ($D \geq 5$ mm) drops to integral rain parameters (concentration, rain rate, and reflectivity) for the averaged drop size distributions. Because minimum size cutoff is 0.6 mm for the UI 2DVD, very small drops contribute only to the JWD spectra. The last size bin of JWD centers at 5.1-mm diameter. Therefore, very large drops contribute much less to the JWD spectra.

Despite the 0.3-mm lower minimum drop size cutoff in JWD, its concentration was lower than that of 2DVD except at very light rain. This result is because the higher concentrations of medium-size drops in 2DVD compensated for the absence of very small drops. At very heavy and extreme rain rates, the higher concentrations of small drops in 2DVD were also a factor. In 2DVD, the small drops were the main contributors (>50%) to the number concentration in very light and light rain. The peak contribution shifted to medium-size drops at moderate rain. The JWD had a similar trend, except that the shift from small- to medium-size drops occurred in heavy rain. For rain rate, the 2DVD had higher readings at all rain-intensity ranges. This result is because the concentration of medium-size drops was higher in 2DVD than in JWD, and the medium-size drops were the main contributors to the rain rate in both disdrometers regardless of rain intensity. For reflectivity, the difference between the 2DVD and JWD reflectivities was less than 1 dB at all rain intensities. In fact, it was less than 0.5 dB except for light rain. Like for the rain rate, the medium-size drops were the main contributors to the reflectivity, except at heavy and extreme rain intensities, for which the large drops were the main contributors.

It is likely that both disdrometers adequately sample medium-size and large drops. The differences at these size regimes could be the result of the differences in sampling volume of the instruments (Campos and Zawadzki 2000). It also is likely that JWDs underestimate the small drops at extreme rain intensities (Fig. 4f). Although only for 9% of the time did rain fall at extreme intensity, it turned out to account for 55% of the total rain.

The composite spectra of JWD and 2DVD that included all coincident observations agreed well with each other (Fig. 5). This result suggests that both disdrometers can be used to investigate the differences in DSD in different climatic regimes. The ability to measure very large drops with 2DVD should be considered a substantial improvement in DSD research. The elimination of small and very small drops due mainly to mismatching in 2DVD observations brings uncertainty about the concentrations of these size drops. This uncertainty potentially may cause an error in DSD parameterizations.

5. DSD parameterization

To parameterize the drop size distribution, the observed spectra are often represented by an exponential or gamma function. The exponential DSD (Waldvogel 1974) is expressed as $N(D) = N_0 \exp(-\Lambda D)$, where N_0 and Λ are the intercept and slope parameters, D is the drop diameter, and $N(D)$ is the drop concentration. The gamma DSD (Ulbrich 1983) is a generalization of the above and has the functional form $N(D) = N_0 D^m \exp(-\Lambda D)$, where m is the shape parameter. The shape parameter of a gamma distribution may be considered to be a measure of deviation from exponential distribution. When $m = 0$, the gamma DSD converges to the exponential DSD. Positive (negative) values of the shape parameter indicate the concave-down (-up) shape of the drop spectrum. Although the lognormal distribution (Feingold and Levin 1986) is also a candidate, the fit does not differ from the gamma DSD much.

We applied the gamma and exponential functions to each of the six composite DSDs at different rain intensities (Fig. 4) and to the overall composite spectra (Fig. 5). We summarize the parameters of gamma distributions in Table 5 and of exponential in Table 6. We used the third, fourth, and sixth moments of the observed spectra (Tokay and Short 1996) to determine the parameters of the gamma distribution. These high-order moments are related to the liquid water content, rain rate, and radar reflectivity, all of which are of interest in cloud modeling and radar rainfall retrieval studies. They are not sensitive to the underestimation of small drops in JWD. We used the third and sixth moments of observed spectra to parameterize the exponential distribution (Waldvogel 1974). To have a more direct comparison between the two disdrometers' DSD parameterization, the minimum drop size cutoff was set to 0.6 mm in JWD.

The parameters of exponential and gamma distributions that we present here were derived from limited samples at six different rain intensities. Therefore, they do not necessarily represent the typical DSD needed for cloud modeling studies. The limited sample may also

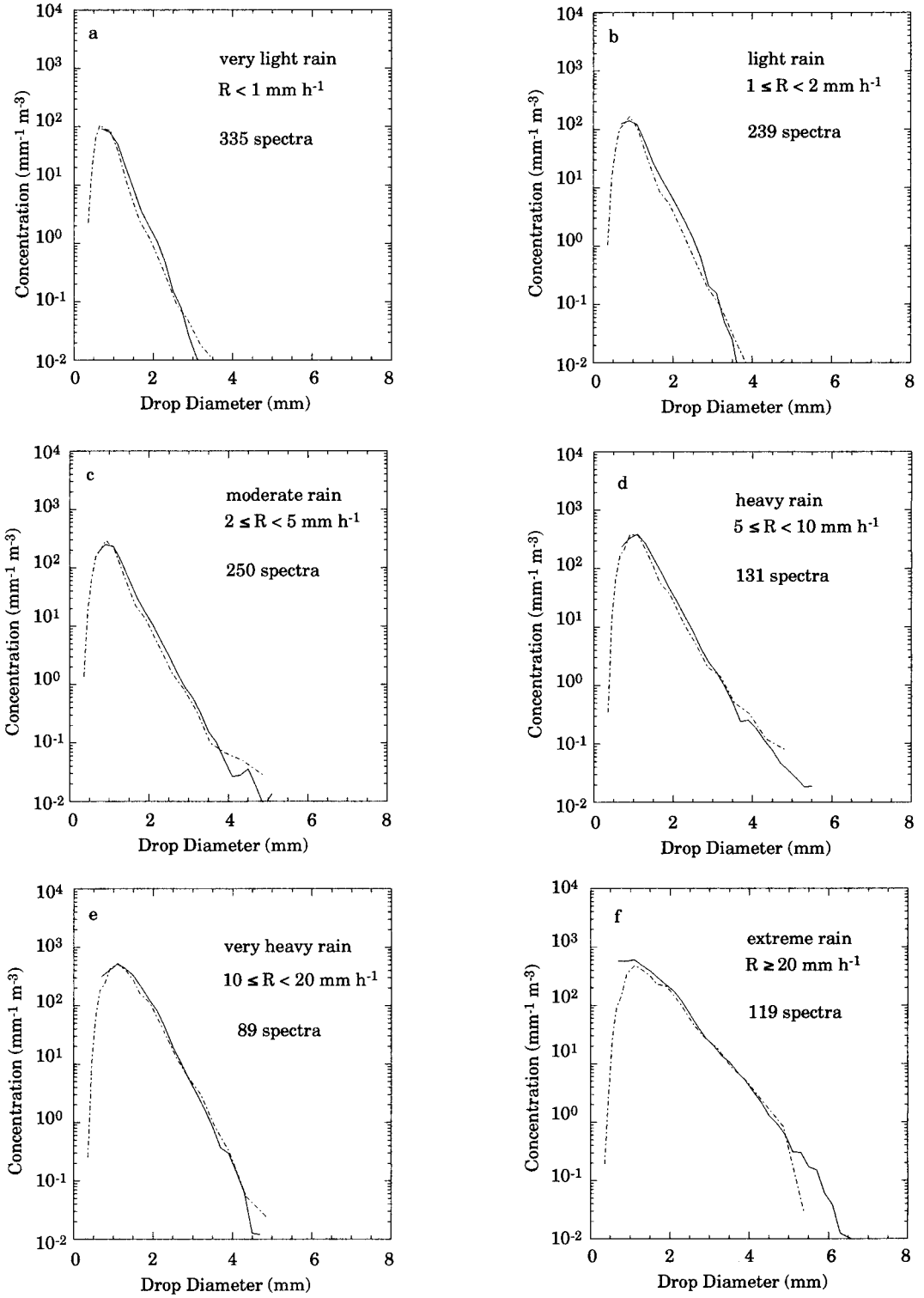

FIG. 4. Averaged drop size distributions for six different rain intensity intervals. The boundaries of rain rate and the number of averaged samples are given. The solid and dash–dotted lines denote 2DVD and JWD, respectively.

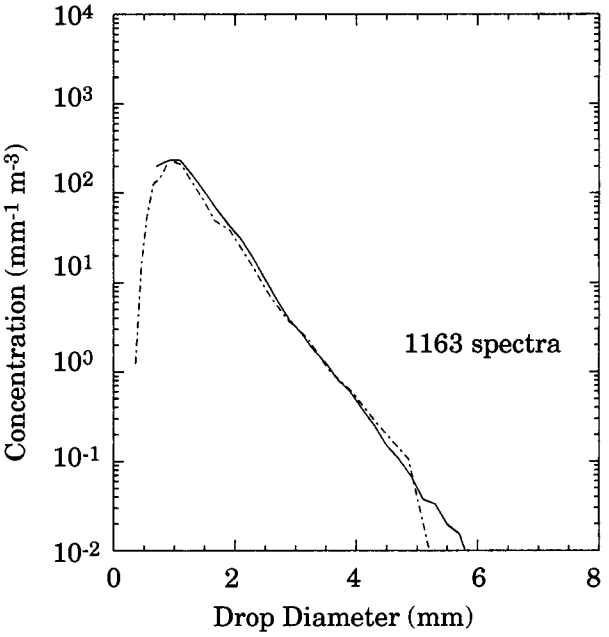

FIG. 5. Averaged drop size distributions for all (1163 1-min) coincident observations of the disdrometers. The solid and dash–dotted lines denote 2DVD and JWD, respectively.

be the reason for the absence of systematic variation between the parameters and rain rate. Sauvageot and Lacaux (1995) showed a systematic increase in intercept and a decrease in slope parameters of exponential distribution with increasing rain rate. Tokay and Short (1996), on the other hand, showed an increase in all three parameters of the gamma distribution with rain rate. We found similar trends using the composite spectra from the entire set of JWD observations, which were about 2.5 times the coincident JWD and 2DVD measurements. Nevertheless, this issue is beyond the scope of this paper.

The parameters of gamma distribution derived from 2DVD spectra were higher than those derived from JWD spectra except at extreme rain intensities (Table 5). Because the fitted distributions are based on high moments of the drop spectra, the population of medium and large drops mainly determines the parameters of gamma distribution. The shape parameter of gamma distribution is a unique function of the $G\ [=X_4^3/X_3^2X_6)]$ factor, where X_3, X_4, and X_6 represent the third, fourth, and sixth moments, respectively, of the spectra. The ratio of the numerator to the denominator in the G factor was higher in 2DVD spectra than in JWD spectra except at extreme rain intensities. This result suggests the presence of more medium-size drops and fewer large drops in 2DVD spectra than in JWD spectra. This case was indeed true at very light rain intensities. As the rain rate increased, more large drops were found in 2DVD spectra than in JWD spectra. However, a large amount of medium-size drops in 2DVD spectra dominated the G factor, even in heavy rain for which very large drops were present in

TABLE 4. Percentage contribution of very small (VS), small (S), medium-size (M), large (L), and very large (VL) drops to total concentration, rain rate, and reflectivity. The boundaries of five size categories are given in the text. The total concentration, rain rate, and reflectivity calculated from composite spectra are also shown outside the parentheses for both types of disdrometers.

Rain intensity (mm h^{-1})	N_{JWD} (m^{-3}) (VS, S, M, L, VL)	N_{2DVD} (m^{-3}) (VS, S, M, L, VL)	R_{JWD} (mm h^{-1}) (VS, S, M, L, VL)	R_{2DVD} (mm h^{-1}) (VS, S, M, L, VL)	Z_{JWD} (dB) (VS, S, M, L, VL)	Z_{2DVD} (dB) (VS, S, M, L, VL)
$R < 1$	59 (15, 65, 20, 0, 0)	52 (0, 67, 33, 0, 0)	0.4 (2, 32, 61, 5, 0)	0.5 (0, 25, 74, 1, 0)	22.3 (0, 7, 51, 42, 0)	21.9 (0, 7, 88, 5, 0)
$1 \leq R < 2$	97 (6, 58, 36, 0, 0)	101 (0, 52, 48, 0, 0)	1.1 (0, 19, 75, 6, 0)	1.4 (0, 13, 85, 2, 0)	27.5 (0, 4, 61, 35, 0)	28.4 (0, 3, 88, 9, 0)
$2 \leq R < 5$	181 (5, 52, 43, 0, 0)	184 (0, 47, 53, 0, 0)	2.6 (0, 14, 76, 10, 0)	3.1 (0, 10, 85, 5, 0)	32.3 (0, 2, 52, 46, 0)	32.8 (0, 2, 70, 26, 2)
$5 \leq R < 10$	282 (3, 39, 57, 1, 0)	312 (0, 36, 64, 0, 0)	6.1 (0, 7, 78, 15, 0)	7.0 (0, 6, 86, 7, 1)	36.9 (0, 1, 47, 52, 0)	37.4 (0, 1, 63, 30, 6)
$10 \leq R < 20$	445 (1, 28, 70, 1, 0)	498 (0, 29, 71, 0, 0)	13.9 (0, 4, 85, 11, 0)	14.7 (0, 3, 92, 5, 0)	40.0 (0, 0, 64, 36, 0)	40.2 (0, 1, 81, 18, 0)
$R \geq 20$	501 (1, 17, 78, 4, 0)	725 (0, 31, 67, 2, 0)	34.6 (0, 1, 62, 37, 0)	35.7 (0, 2, 72, 24, 2)	47.2 (0, 0, 27, 72, 1)	47.6 (0, 0, 37, 52, 11)
All	192 (4, 38, 57, 1, 0)	223 (0, 39, 60, 1, 0)	6.2 (0, 5, 69, 26, 0)	6.6 (0, 4, 79, 16, 1)	38.6 (0, 0, 34, 65, 1)	39.0 (0, 0, 46, 45, 9)

TABLE 5. Gamma DSD–fit parameters for JWD and 2DVD.

Rain intensity (mm h^{-1})	No. of 1-min DSD samples	N_{02DVD} (m^{-3} mm^{-1-m})	Λ_{2DVD} (mm^{-1})	m_{2DVD}	N_{0JWD} (m^{-3} mm^{-1-m})	Λ_{JWD} (mm^{-1})	m_{JWD}
$R < 1$	335	21 638	6.04	3.6	546	2.85	−0.5
$1 \le R < 2$	239	15 429	4.98	3.2	2103	3.27	0.5
$2 \le R < 5$	250	6345	3.51	1.5	2565	2.79	0.2
$5 \le R < 10$	131	8429	3.20	1.4	4279	2.71	0.6
$10 \le R < 20$	89	93 882	5.24	5.2	39 750	4.44	3.9
$R \ge 20$	119	8144	2.56	1.8	7038	2.85	2.7
All	1163	2747	2.53	1.0	2117	2.49	1.0

the 2DVD DSD (Fig. 4d). At extreme rain intensities, the presence of very large drops became a factor, and a higher G factor was observed in the JWD spectrum (Fig. 4f). The intercept parameter of the gamma distribution is related to the shape parameter (Ulbrich 1983), and, therefore, it displayed similar behavior. The slope parameter is expressed as $\Lambda = (m + 4)/D_m$, where D_m ($=X_4/X_3$) is the mass-weighted drop diameter. Although the mass-weighted drop diameter was lower in JWD spectra at the lowest three rain intensities, the numerator dominated at all rain intensities, resulting in higher Λ in 2DVD spectra than in JWD spectra (Table 5). When we combined all the coincident observations of JWD and 2DVD, a good agreement in gamma parameters was evident, which demonstrates that the gamma parameters that were derived from long-term observations of JWD represent the characteristic of DSD in a climatic regime and are instrument-independent.

The parameters of exponential distribution were higher in 2DVD spectra than in JWD, regardless of rain intensity (Table 6). The slope parameter, which is a function of H ($=X_3/X_6$) factor, depends mainly on the ratio of medium- to large-size drops. In the presence of very large drops, this ratio is shifted from medium to large drops and form large to very large drops. At all rain intensities, the H factor of 2DVD was close to the H factor of JWD, indicating a very good agreement between the slope parameter of JWD spectra and that of 2DVD spectra. This was also evident through the ratios of Λ_{2DVD} to Λ_{JWD} in Table 6. The intercept parameters of both disdrometers also had a good agreement. The ratio of N_{2DVD} to N_{JWD} was less than 1.4 except at very light rain intensities. These comparisons increase the confidence in DSD parameterization in exponential form that was previously developed from long-term observations of JWD (e.g., Sauvageot and Lacaux 1995).

6. Relations between integral parameters

The relations between reflectivity and rain rate, reflectivity and liquid water content, and reflectivity and attenuation were derived by employing 1163 coincident DSD measurements of JWD and UI 2DVD. For the first two pairs, we derived two sets of relations, one for S band and one for the TRMM precipitation radar (Ku band). Although our main objective was to investigate the instrument dependency of three pairs of relations, we also examined the dependency of these relations on the regression technique (Campos and Zawadzki 2000; Ciach and Krajewski 1999). Table 7 presents relations between Z and R and Z_e and R for reflectivity and rain rate as a dependent variable, for linear and nonlinear regression, and for JWD and 2DVD measurements. As described above, Z denotes the reflectivity at S band, and reflectivity at Ku band is denoted as Z_e. The pairs of A, b and A', b' that were directly derived from regression analysis are denoted in bold face type. The chi-square errors of rain rate X_R^2 are also given in units of millimeter per hour. Table 8 is constructed similarly to Table 7 but for liquid water content. The chi-square errors of liquid water content X_M^2 are in units of grams per cubic meter.

The relations between reflectivity and rain rate traditionally are derived from a linear regression in which rain rate is an independent variable (Battan 1973). The linear regression is performed by minimizing chi-square error statistics between ln(R) and ln(Z). Rain rate is derived operationally from reflectivity. Hence, rain rate

TABLE 6. Exponential DSD–fit parameters for JWD and 2DVD.

Rain intensity (mm h^{-1})	No. of 1-min DSD samples	N_{02DVD} (m^{-3} mm^{-1})	Λ_{2DVD} (mm^{-1})	N_{0JWD} (m^{-3} mm^{-1})	Λ_{JWD} (mm^{-1})	N_{02DVD}/N_{0JWD}	$\Lambda_{2DVD}/\Lambda_{JWD}$
$R < 1$	335	1408	3.50	790	3.18	1.78	1.10
$1 \le R < 2$	239	2100	2.99	1496	2.94	1.40	1.02
$2 \le R < 5$	250	2913	2.71	2266	2.66	1.28	1.02
$5 \le R < 10$	131	4468	2.48	3291	2.41	1.36	1.03
$10 \le R < 20$	89	9826	2.53	7850	2.47	1.25	1.02
$R \ge 20$	119	6149	1.86	4986	1.83	1.23	1.02
All	1163	2063	2.11	1613	2.07	1.28	1.02

TABLE 7. Relations between radar reflectivity and rain rate. Different sets of relations are derived considering reflectivity at Rayleigh and Mie regimes. Chi-square errors between rain rate that is directly calculated from observed spectra R_t and rain rate that is derived from reflectivity–rain-rate relation (in boldface) R_p are also given.

Disdrometer (least squares fit)	$Z = AR^b$ (A, b)	$R = A' Z^{b'}$ (A', b')	X^2 error $\Sigma(R_p - R_t)^2$	$Z_e = AR^b$ (A, b)	$R = A' Z_e^{b'}$ (A', b')	X^2 error $\Sigma(R_p - R_t)^2$
JWD (linear)	**302, 1.37**	0.015, 0.73	39 523	**311, 1.45**	0.019, 0.69	70 016
JWD (linear)	283, 1.48	**0.022, 0.67**	20 544	282, 161	**0.030, 0.62**	25 415
JWD (nonlinear)	**265, 1.47**	0.022, 0.68	22 207	**299, 1.57**	0.026, 0.64	28 723
JWD (nonlinear)	141, 1.67	**0.052, 0.60**	19 048	127, 1.84	**0.072, 0.54**	23 837
2DVD (linear)	**309, 1.38**	0.016, 0.72	42 684	**312, 1.45**	0.019, 0.69	83 702
2DVD (linear)	275, 1.51	**0.024, 0.66**	24 698	266, 1.64	**0.033, 0.61**	29 878
2DVD (nonlinear)	**206, 1.55**	0.032, 0.65	27 803	**230, 1.63**	0.036, 0.61	31 619
2DVD (nonlinear)	120, 1.73	**0.063, 0.58**	22 199	104, 1.90	**0.087, 0.53**	27 647

that is converted from a *Z–R* relation differs from the rain rate that is directly derived from *R–Z* regression. The differences between the two methods are large enough to represent two different climatic regimes (Table 7). The chi-square errors in Table 7 exhibit lower values for *R–Z* regression than for *Z–R* regression. This result suggests that rain rate rather than reflectivity should be the dependent variable in regression analysis.

In linear regression, both reflectivity and rain rate are treated in a compressed scale. For instance, the rain rate, which varies between 0.1 and 100 mm h^{-1} in linear scale, is confined to 30 dBR [$=10\log(R)$] dynamic range in a logarithmic scale. Because light rainfall occurs most of the time, the linear regression is weighted toward light rainfall. The *R–Z* that is derived from linear regression produces an accurate representation of the relationship at light rain rates but not necessarily at heavier rain rates (Fig. 6). The nonlinear regression, on the other hand, seeks to minimize the chi-square error in *R–Z* space. It is weighted toward heavy rainfall and tends to overestimate the light rain rates. Therefore, the nonlinear regression produces better rain totals with smaller chi-square errors. The differences between linear and nonlinear *R–Z* regressions are again large enough to represent two different climatic regimes (Table 7).

The discussion presented above demonstrates that the relationship between reflectivity and rain rate is method-dependent. Campos and Zawadzki (2000), who studied instrument uncertainties in *Z–R* relations, showed the dependence of the *Z–R* relations on the regression technique and on the choice of independent variable. They also found that the *Z–R* relations are highly instrument-dependent. Campos and Zawadzki's study was based on a relatively small sample of DSD for rain rates of 0.1–8 mm h^{-1} in a stratiform rain event. However, in our study, comparison of reflectivity and rain-rate relations derived from JWD and 2DVD measurements shows a good agreement (Table 7). The rain-rate difference, based on the instrument *Z–R* relations, is insignificant ($\Delta R < 3$ mm h^{-1}) except $Z > 52$ dB (Fig. 7). The rain-rate difference, based on the choice of independent variable in the *Z–R* relations, becomes a factor ($\Delta R > 3$ mm h^{-1}) at 43 dBZ and becomes increasingly important at higher reflectivities. The rain-rate difference, based on the type of regression technique used in the *Z–R* relations, exceeds 3 mm h^{-1} at $43 < Z < 47$ dB and again at $Z > 55$ dB. Figure 7 is constructed from selected *Z–R* and *R–Z* relations given in columns 2 and 3 of Table 7, respectively. These findings can be carried out for the remainder of the *Z–R* relations in Table 7 and the *Z–M* relations in Table 8.

The relations between reflectivity and rain rate and between reflectivity and liquid water content for the TRMM precipitation radar result in lower rain rates than their counterparts for the S-band radar. This is because reflectivity at the TRMM precipitation-radar wavelength is higher than the reflectivity at S band. The bias is 0.3 dB for all measurements of JWD but becomes 0.9 and

TABLE 8. Relations between radar reflectivity and liquid water content. Different sets of relations are derived considering reflectivity at Rayleigh and Mie regimes. Chi-square errors between liquid water content that is directly calculated from observed spectra M_t and liquid water content that is derived from reflectivity–liquid-water-content relation (in boldface) M_p are also given.

Disdrometer (least squares fit)	$Z = AM^b$ (A, b)	$M = A'Z^{b'}$ (A', b')	X^2 error $\Sigma(M_p - M_t)^2$	$Z_e = AM^b$ (A, b)	$M = A' Z_e^{b'}$ (A', b')	X^2 error $\Sigma(M_p - M_t)^2$
JWD (linear)	**19 639, 1.45**	1.11×10^{-3}, 0.69	130	**25 578, 1.53**	1.33×10^{-3}, 0.65	178
JWD (linear)	32 739, 1.67	**2.01×10^{-3}, 0.60**	45	50 285, 1.83	**2.67×10^{-3}, 0.55**	55
JWD (nonlinear)	**26 755, 1.59**	1.64×10^{-3}, 0.63	53	**41 256, 1.70**	1.91×10^{-3}, 0.59	65
JWD (nonlinear)	28 523, 1.91	**4.61×10^{-3}, 0.52**	43	44 335, 2.11	**6.34×10^{-3}, 0.47**	51
2DVD (linear)	**17 994, 1.39**	0.88×10^{-3}, 0.72	219	**22 429, 1.46**	1.07×10^{-3}, 0.68	291
2DVD (linear)	27 947, 1.61	**1.71×10^{-3}, 0.62**	71	40 500, 1.75	**2.33×10^{-3}, 0.57**	85
2DVD (nonlinear)	**22 739, 1.61**	1.94×10^{-3}, 0.62	76	**33 159, 1.70**	2.18×10^{-3}, 0.59	101
2DVD (nonlinear)	24 365, 1.90	**5.00×10^{-3}, 0.52**	65	38 583, 1.93	**4.23×10^{-3}, 0.52**	79

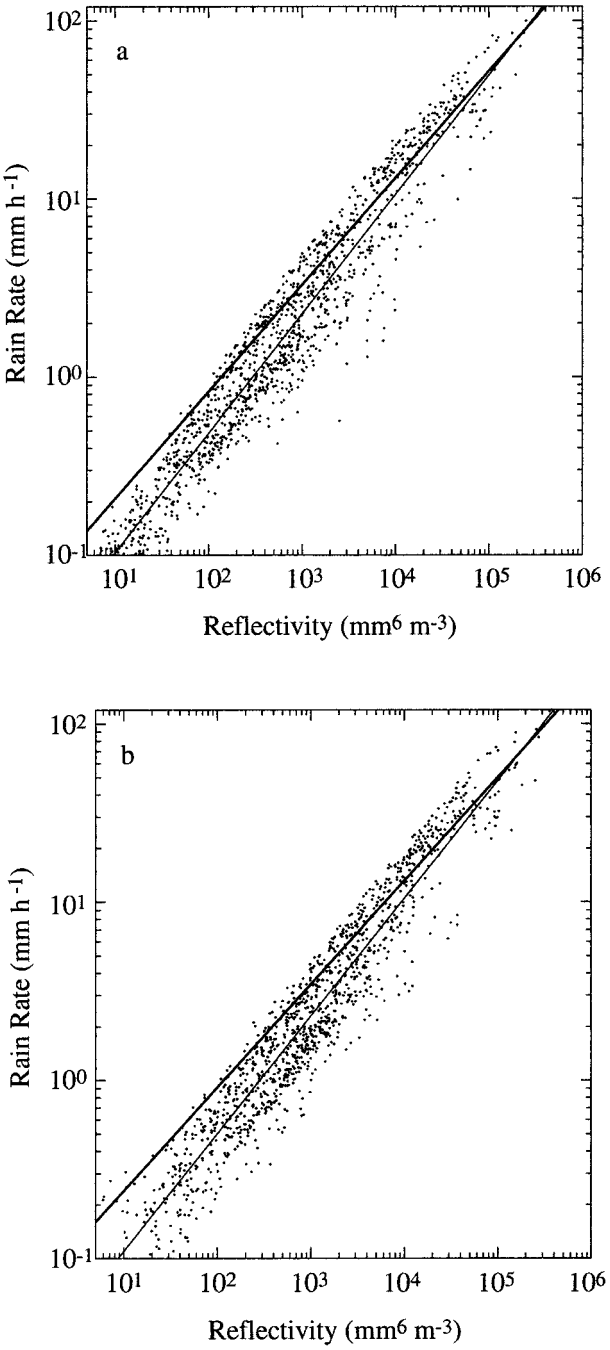

FIG. 6. Reflectivity (Rayleigh regime) vs rain rate for all coincident observations of (a) JWD and (b) 2DVD. The thin line represents the best-fitted curve through linear *R–Z* regression. The thick line shows the best-fitted curve through nonlinear *R–Z* regression.

2.1 dB for the measurements of $Z > 27$ dBZ and of $Z > 44$ dBZ, respectively (Fig. 8). The 2DVD reflectivity measurements exhibit similar biases. Bolen and Chandrasekar (2000) also noted that Ku-band reflectivity can be up to 2 dB higher than S-band reflectivity for the same DSD. At the TRMM precipitation-radar wavelength, attenuation becomes a factor and *A–Z* relations

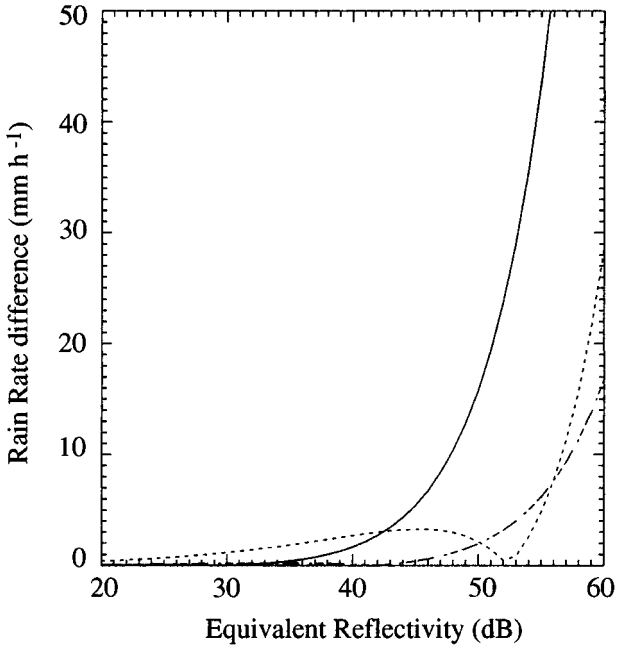

FIG. 7. Absolute differences of rain rate as a function of reflectivity. The difference in rain rate is due to the choice of independent variable (solid), to regression technique (dashed), and to two different types of disdrometers (dash–dotted).

are required for the attenuation correction. Here, $A = 3.06 \times 10^{-4}Z^{0.77}$ and $A = 2.85 \times 10^{-4}Z^{0.79}$ relations are found from the coincident JWD and 2DVD measurements, respectively.

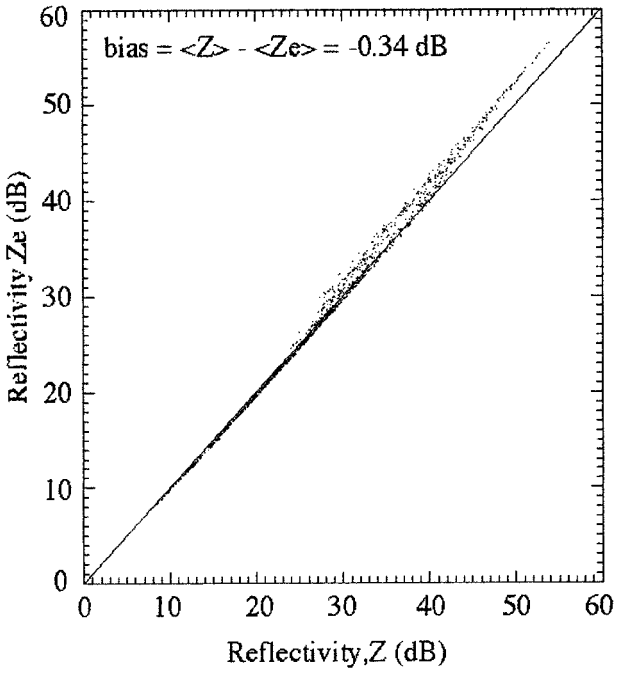

FIG. 8. Reflectivity at S band vs reflectivity at TRMM precipitation radar (Ku band). The bias also is shown.

7. Summary and conclusions

The experimental setup at the master site of the dense rain gauge network in TEFLUN-B provided a unique opportunity to study the characteristics of DSD and its role with respect to radar rainfall measurements. At the master site, two 2DVDs, a JWD, and eight tipping-bucket rain gauges were located within an area of about 100 m $\times$ 50 m. In this study, we first examined the performance of the video- and impact-types of disdrometers by comparing their rain totals with nearby rain gauges. Both types of disdrometers underestimated the rain total, but the agreement was better between the video disdrometer and the rain gauges. The lack of small- to medium-size drops in the DSD was considered to be the main reason for the underestimation of rain by both disdrometers.

To compare with each other, the coincident measurements of drop size distribution by disdrometers were averaged for three scales: a selected time window of a rain event, six rain intensities, and the overall observations. For the last two scales, the averaging was not performed for the NASA 2DVD because of an insufficient number of samples. A good agreement was found between the disdrometers' measurements at all three scales. Given the shortcomings of both impact and video disdrometers, this result was unexpected. It specifically was interesting to observe the absence of an exponential increase toward smaller drop sizes in video disdrometers at rain rates less than 20 mm h^{-1}. The concentration of small drops remained relatively constant or decreased toward the first reliable size interval (0.6–0.8 mm) of the video disdrometer. At $R \geq 20$ mm h^{-1}, the difference between the spectra of the two disdrometers was significant at both the small- and large-size ends of the spectra. Many more small drops were measured by the video disdrometer. Very large drops that were beyond the JWD maximum size limit were present in the 2DVD spectra. Despite these differences, rain rate and reflectivity were within 3% and 0.4 dB, respectively. At light and moderate rain rates, more medium-size drops were observed in 2DVD spectra than in JWD spectra. This observation would result in higher rain rates in 2DVD spectra. The reflectivities that we calculated from 2DVD spectra were also higher than those in JWD spectra except at very light rain. The differences in reflectivity, however, were less than 1 dB.

We fitted the exponential and gamma distributions to the averaged drop size distributions of JWD and of 2DVD. We performed the averaging for the six rain intensity intervals and for all the observations. The parameters of both exponential and gamma distributions were mostly higher in 2DVD spectra than in JWD spectra. This result was due to the presence of more medium-size drops in 2DVD spectra, even though the presence of very large drops also played a role. When all the coincident DSD measurements of JWD and of 2DVD were averaged, a very good agreement was found between the parameters of exponential and gamma distributions. This agreement suggests that the parameters of exponential and gamma distribution are not instrument-dependent.

The relations between reflectivity and rain rate, reflectivity and liquid water content, and reflectivity and attenuation were derived for S-band and Ku-band radars. We found a good agreement between the relations derived from two types of disdrometers. This agreement indicates that these relations are instrument insensitive. Rather, we found them to be sensitive to the method of regression and to the choice of independent variable. The nonlinear regression is a better estimate of heavy rainfall but not of light rain. The nonlinear regression consequently results in more accurate rain totals and lower chi-square errors between the observed and predicted integral parameters. Because rain rate is derived from radar reflectivity measurements, the rain rate should be selected as a dependent variable. This selection results in lower chi-square errors. The relations derived for S-band and Ku-band radars differ from each other. This difference is because the reflectivity at the S band is lower than reflectivity at Ku-band in high-reflectivity regions.

Although we collected many more samples of simultaneous measurements of DSD by video and impact disdrometers than have previous studies, we still need to conduct longer-term experiments in which both types of disdrometers operate side by side. During TEFLUN-B, the late arrival of the NASA video disdrometer unit and the overheating problems were the main reasons for the limited sample of coincident observations. Longer observations will provide more robust DSD parameterization at different rain intensities and would also allow us to examine the instrument-dependency of the relations between integral parameters for different precipitation types. An attempt to accomplish this goal is under way at the NASA Wallops Flight Facility.

Acknowledgments. The authors thank Mr. Otto Thiele, former head of the NASA TRMM Office, and Dr. Edward Zipser of the University of Utah for their vision and leadership during the TEFLUN-B field campaign. We also extend thanks to Drs. Kenneth Gage and Christopher Williams of NOAA Aeronomy Laboratory for their operational responsibilities with the Joss–Waldvogel disdrometer and for providing tipping-bucket rain gauge data. We acknowledge the assistance of Paul Kucera and Emad Habib of the Iowa Institute of Hydraulic Research and students of University of Central Florida who all operated the disdrometer and rain gauge network during the field campaign. Special thanks go to Rhonie Chamberlain of Computer Science Corporation for her efforts in analyzing the NASA 2D video disdrometer data. This study was sponsored by NASA's TRMM program through Grants NAG5-9664 and NCC5-339 under Dr. Ramesh Kakar, Program Scientist.

REFERENCES

Barthazy, E., W. Henrich, and A. Waldvogel, 1998: Size distribution of hydrometeors through the melting layer. *Atmos. Res.,* **47–48,** 193–208.

Battan, L. J., 1973: *Radar Observation of the Atmosphere*. University of Chicago Press, 324 pp.

Bolen, S. M., and V. Chandrasekar, 2000: Quantitative cross validation of space-based and ground-based radar observations. *J. Appl. Meteor.,* **39,** 2071–2079.

Campos, E., and I. Zawadzki, 2000: Instrument uncertainties in *Z–R* relations. *J. Appl. Meteor.,* **39,** 1088–1102.

Ciach, G. J., and W. F. Krajewski, 1999: Radar–rain gauge comparison under observational uncertainties. *J. Appl. Meteor.,* **38,** 1519–1525.

Donnadieu, G., 1980: Comparison of results obtained with the VIDIAZ spectropluviometer and the Joss-Waldvogel rainfall disdrometer in a ''rain of thunder type.'' *J. Appl. Meteor.,* **19,** 593–597.

Feingold, G., and Z. Levin, 1986: The lognormal fit to raindrop spectra from frontal convective clouds in Israel. *J. Climate Appl. Meteor.,* **25,** 1346–1363.

Ferrier, B. S., W.-K. Tao, and J. Simpson, 1995: Double-moment multiple-phase four-class bulk ice scheme. Part II: Simulations of convective storms in different large-scale environments and comparisons with other bulk parameterizations. *J. Atmos. Sci.,* **52,** 1001–1033.

Gunn, R., and G. D. Kinzer, 1949: The terminal velocity of fall for water drops in stagnant air. *J. Meteor.,* **6,** 243–248.

Habib, E., W. F. Krajewski, V. Nešpor, and A. Kruger, 1999: Numerical simulation studies of raingage data correction due to wind effect, *J. Geophys. Res.,* **104,** 19 723–19 734.

——, ——, and A. Kruger, 2001: Sampling errors of fine resolution tipping-bucket rain gauge measurements. *J. Hydrol. Eng.,* **6,** 159–166.

Hauser, D., P. Amayenc, B. Nutten, and P. Waldteufel, 1984: A new optical instrument for simultaneous measurements of raindrop diameter and fall distribution. *J. Atmos. Oceanic Technol.,* **1,** 256–269.

Hong, Y., C. D. Kummerow, and W. S. Olson, 1999: Separation of convective and stratiform precipitation using microwave brightness temperature. *J. Appl. Meteor.,* **38,** 1195–1213.

Hosking, J. G., and C. D. Stow, 1991: Ground-based measurements of raindrop fallspeeds. *J. Atmos. Oceanic Technol.,* **8,** 137–147.

Jones, D. M. A., 1992: Raindrop spectra at the ground. *J. Appl. Meteor.,* **31,** 1219–1225.

Joss, J., and A. Waldvogel, 1967: Ein Spectrograph für Niederschlagstropfen mit automatisher Auswertung (A spectrograph for the automatic analysis of raindrops). *Pure Appl. Geophys.,* **68,** 240–246.

——, and E. G. Gori, 1976: The parameterization of raindrop size distributions. *Riv. Ital. Geofis.,* **3,** 273–283.

Knollenberg, R. G., 1970: The optical array: An alternative to scattering or extinction for airborne particle size distribution. *J. Appl. Meteor.,* **9,** 86–103.

Kummerow, C., W. Barnes, T. Kozu, J. Shiue, and J. Simpson, 1998: The Tropical Rainfall Measuring Mission (TRMM) sensor package. *J. Atmos. Oceanic Technol.,* **15,** 809–817.

Laws, J. O., and D. A. Parsons, 1943: The relation of raindrop size to intensity. *Trans. Amer. Geophys. Union,* **24,** 452–460.

Loffler-Mang, M., and J. Joss, 2000: An optical disdrometer for measuring size and velocity of hydrometeors. *J. Atmos. Oceanic Technol.,* **17,** 130–139.

Marshall, J. S., and W. McK. Palmer, 1948: The distribution of raindrops with size. *J. Meteor.,* **5,** 165–166.

——, R. C. Langille, and W. McK. Palmer, 1947: Measurement of rainfall by radar. *J. Meteor.,* **4,** 186–192.

McFarquhar, G. M., and R. List, 1993: The effect of curve fits for the disdrometer calibration on raindrop spectra, rainfall rate, and radar reflectivity. *J. Appl. Meteor.,* **32,** 774–782.

Nešpor, V., W. F. Krajewski, and A. Kruger, 2000: Wind-induced error of rain drop size distribution measurement using a two-dimensional video disdrometer. *J. Atmos. Oceanic Technol.,* **17,** 1483–1492.

Sauvageot, H., and J.-P. Lacaux, 1995: The shape of averaged drop size distributions. *J. Atmos. Sci.,* **52,** 1070–1083.

Schönhuber, M., H. E. Urban, J. P. V. Poiares Baptista, W. L. Randeu, and W. Riedler, 1997: Weather radar versus 2D-video-disdrometer data. *Weather Radar Technology for Water Resources Management,* B. Braga Jr. and O. Massambani, Eds., UNESCO Press, 159–171.

Schuur, T. J., A. Ryzhkov, and D. S. Zrnić, 2001: Drop size distributions measured by a 2D video disdrometer: Comparison with dual-polarization radar study. *J. Appl. Meteor.,* **40,** 1019–1034.

Sheppard, B. E., 1990: Effect of irregularities in the diameter classification of raindrop by Joss–Waldvogel disdrometer. *J. Atmos. Oceanic Technol.,* **7,** 180–183.

——, and P. I. Joe, 1994: Comparison of raindrop size distribution measurements by a Joss–Waldvogel disdrometer, a PMS 2DG spectrometer, and a POSS Doppler radar. *J. Atmos. Oceanic Technol.,* **11,** 874–887.

Stow, C. D., and K. Jones, 1981: A self evaluating disdrometer for the measurement of raindrop size and charge at the ground. *J. Appl. Meteor.,* **20,** 1160–1176.

Tokay, A., and D. A. Short, 1996: Evidence from tropical raindrop spectra of the origin of rain from stratiform versus convective clouds. *J. Appl. Meteor.,* **35,** 355–371.

——, O. W. Thiele, A. Kruger, and W. F. Krajewski, 1999: New measurements of drop size distribution and its impact on radar rainfall retrievals. Preprints, *29th Conf. on Radar Meteorology,* Montreal, QC, Canada, Amer. Meteor. Soc., 659–662.

Ulbrich, C. W., 1983: Natural variations in the analytical form of the raindrop size distribution. *J. Climate Appl. Meteor.,* **22,** 1764–1775.

Waldvogel, A., 1974: The N_0 jump of raindrop spectra. *J. Atmos. Sci.,* **31,** 1068–1078.